Haldane phase in one-dimensional topological Kondo insulators

Alejandro Mezio, Alejandro M. Lobos,* Ariel O. Dobry, and Claudio J. Gazza
Facultad de Ciencias Exactas, Ingeniería y Agrimensura, Universidad Nacional de Rosario, and Instituto de Física Rosario (CONICET), Bv. 27 de Febrero 210 bis, 2000 Rosario, Argentina

(Received 1 September 2015; revised manuscript received 5 November 2015; published 24 November 2015)

We investigate the ground-state properties of a recently proposed model for a topological Kondo insulator in one dimension (i.e., the p-wave Kondo-Heisenberg lattice model) by means of the density-matrix renormalization-group method. The nonstandard Kondo interaction in this model is different from the usual (i.e., local) Kondo interaction in that the localized spins couple to the "p-wave" spin density of conduction electrons, inducing a topologically nontrivial insulating ground state. Based on the analysis of the charge- and spin-excitation gaps, the string order parameter, and the spin profile in the ground state, we show that, at half filling and low energies, the system is in the Haldane phase and hosts topologically protected spin-1/2 end states. Beyond its intrinsic interest as a useful "toy model" to understand the effects of strong correlations on topological insulators, we show that the p-wave Kondo-Heisenberg model could be experimentally implemented in p-band optical lattices loaded with ultracold Fermi gases.

DOI: 10.1103/PhysRevB.92.205128 PACS number(s): 71.27.+a, 75.30.Mb, 75.10.Pq, 75.10.Kt

I. INTRODUCTION

Topological insulators are a new class of materials, first proposed theoretically for two- and three-dimensional systems with time-reversal symmetry [1–3], and soon after found in experiments on HgTe quantum wells [4], and in $Bi_{1-x}Sb_x$ [5] and Bi_2Se_3 [6]. Despite displaying an insulating behavior in the bulk, these materials support topologically protected gapless edge modes which are robust against local perturbations as long as time-reversal symmetry is preserved (e.g., nonmagnetic disorder). More specifically, the electronic structure of a topological insulator cannot be smoothly connected to that of a trivial insulator, a fact that is mathematically expressed in the existence of a nonzero topological "invariant," an integer number quantifying the topological order in the ground state. A complete classification based on the underlying symmetries has been achieved in the form of a "periodic table of topological insulators" [7–9]. Nevertheless, this classification refers only to the gapped phases of noninteracting fermions, and leaves open the problem of characterizing and classifying strongly interacting topological insulators. This is a very important open question in modern condensed-matter physics.

On the other hand, topological Kondo insulators (TKIs) are a type of recently proposed materials where strong interactions and topology naturally coexist [10–12]. Within a mean-field picture [13–15], TKIs can be understood as a strongly renormalized f electron band lying close to the Fermi level, and hybridizing with the conduction-electron d bands. At half filling, an insulating state appears due to the opening of a low-temperature hybridization gap at the Fermi energy induced by interactions. Due to the opposite parities of the states being hybridized, a topologically nontrivial ground state emerges, characterized by an insulating gap in the bulk and conducting Dirac states at the surface. At present, TKI materials, among which samarium hexaboride (SmB_6) is the best known example, are under intense investigation both theoretically and experimentally [16–19].

In order to gain further intuition into the effect of strong interactions, recently Alexandrov and Coleman [20] proposed an analytically tractable model for a one-dimensional (1D) TKI, i.e., the "p-wave" Kondo-Heisenberg model (p-KHM), consisting of a chain of spin-1/2 magnetic impurities interacting with a half-filled one-dimensional electron gas through a Kondo exchange [see Fig. 1(a)]. The peculiarity of this model, which makes it crucially different from other one-dimensional Kondo lattice models studied previously [21–32], is that the Kondo exchange couples to the "p-wave" conduction-electron spin density, allowing for effective next-nearest-neighbor hopping processes in the conduction band accompanied by a spin flip. Using a standard mean-field description [13–15], the above authors found a topologically nontrivial insulating ground state (i.e., topological class D [7–9]) which hosts magnetic states at the open ends of the chain. Soon after, two of us studied this system using the Abelian bosonization approach combined with a perturbative renormalization-group analysis, revealing an unexpected connection to the Haldane phase at low temperatures [33]. The Haldane phase is a paradigmatic example of a strongly interacting topological system, with unique features such as topologically protected spin-1/2 end states, nonvanishing string order parameter, and the breaking of a discrete $Z_2 \times Z_2$ hidden symmetry in the ground state [34–36]. The striking results in Ref. [33] indicate that 1D TKI systems might be much more complex and richer than expected with the naïve mean-field approach, and suggest that they must be reconsidered from the more general perspective of interacting symmetry-protected topological (SPT) phases [37–39].

However, despite describing correctly the universal low-energy behavior of 1D TKI systems, the bosonization technique used in Ref. [33] cannot provide a quantitative description of the physical observables, nor it accounts for the nonuniversal behavior arising from the specificity of the p-KHM. In addition, these results are strictly valid in the limit of small Kondo exchange (J_K), where the perturbation approach is applicable. Therefore, it becomes necessary to analyze the properties of the p-KHM with an independent and unbiased technique, which allows us to explore a broader range

*Electronic address: lobos@ifir-conicet.gov.ar

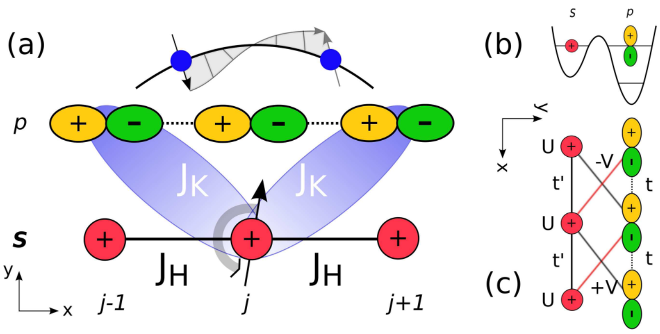

FIG. 1. (Color online) (a) Representation of the p-wave Kondo-Heisenberg model (p-KHM) in one dimension. Upper leg represents the conduction electron p band, and lower leg corresponds to a spin-1/2 Heisenberg chain. The Kondo exchange J_K couples a spin $\mathbf{S}_j$ with the p-wave spin density in the conduction band [see Eq. (3)]. (b) Microscopic model effectively realizing the p-KHM at low energies, and allowing an experimental implementation in p-band optical lattices. The direct hopping across a given rung vanishes due to the different parities of the orbitals.

of parameters of the model and to corroborate the results of bosonization. This is the main goal of this work.

In this paper we study the ground-state properties of the finite-length p-KHM in one dimension using the density-matrix renormalization group (DMRG) [40,41]. Our results indicate that the system is a Haldane insulator with protected spin-1/2 end states and finite string order parameter, therefore supporting the predictions of Ref. [33]. We also propose that this exotic model could be realized in p-band optical lattices loaded with ultracold Fermi gases, which would allow for controlled experimental studies of TKIs in the laboratory.

The paper is organized as follows. In Sec. II we present the model and give some details on the DMRG algorithm used to solve it. In Secs. III and IV we perform a detailed finite-size scaling analysis to study the charge and spin gap in the thermodynamical limit. In Sec. III we show that the system develops a Mott-insulating gap, even in absence of a Hubbard U interaction in the electronic chain, and in Sec. IV we show the appearance of topologically protected spin-1/2 states at the ends of the chain. In Sec. V we compute the string order parameter [see Eq. (7)], whose nonzero expectation value is a hallmark of the Haldane phase. In Sec. VI we discuss a possible physical realization of this model using cold Fermi atoms trapped in an optical lattice. Finally in Sec. VII we give a summary and the conclusions of this work.

II. MODEL

The Hamiltonian of the p-KHM is $H = H_1 + H_2 + H_K$ [20], where the conduction band is represented by a L-site tight-binding chain

$$H_1 = -t \sum_{j=1,\sigma}^{L-1} (p_{j,\sigma}^\dagger p_{j+1,\sigma} + \text{H.c.}), \tag{1}$$

with $p_{j,\sigma}^\dagger$ the creation operator of an electron with spin σ at site j with spatial p symmetry [upper leg in Fig. 1(a)]. The Hamiltonian

$$H_2 = J_H \sum_{j=1}^{L-1} \mathbf{S}_j \cdot \mathbf{S}_{j+1} \quad (J_H > 0) \tag{2}$$

[bottom leg in Fig. 1(a)] corresponds to a spin-1/2 Heisenberg chain, and H_K is the Kondo exchange coupling between H_1 and H_2 [20],

$$H_K = J_K \sum_{j=1}^{L} \mathbf{S}_j \,.\, \boldsymbol{\pi}_j, \tag{3}$$

with $J_K > 0$. This Kondo interaction is unusual in that it couples the spin $\mathbf{S}_j$ in the Heisenberg chain to the "p-wave" spin density in the fermionic chain at site j, defined as

$$\boldsymbol{\pi}_j \equiv \sum_{\alpha,\beta} \left(\frac{p_{j+1,\alpha}^\dagger - p_{j-1,\alpha}^\dagger}{\sqrt{2}} \right) \left(\frac{\boldsymbol{\sigma}_{\alpha\beta}}{2} \right) \left(\frac{p_{j+1,\beta} - p_{j-1,\beta}}{\sqrt{2}} \right), \tag{4}$$

where the notation $p_{0,\sigma} = p_{L+1,\sigma} = 0$ is implied, and where $\boldsymbol{\sigma}_{\alpha\beta}$ is the vector of Pauli matrices. Equation (3) can be written as $H_K = H_K^{(1)} + H_K^{(2)}$, where

$$H_K^{(1)} = \frac{J_K}{2} \sum_j \mathbf{S}_j \,.\, (\mathbf{s}_{j-1} + \mathbf{s}_{j+1}) \tag{5}$$

contains the coupling of a localized spin $\mathbf{S}_j$ with the usual spin density at site $j \pm 1$ in the conduction band [here $\mathbf{s}_j = \sum_{\alpha,\beta} p_{j,\alpha}^\dagger (\frac{\boldsymbol{\sigma}_{\alpha\beta}}{2}) p_{j,\beta}$], and

$$H_K^{(2)} = -\frac{J_K}{2} \sum_j \mathbf{S}_j \cdot \left[\sum_{\alpha,\beta} p_{j+1,\alpha}^\dagger \left(\frac{\boldsymbol{\sigma}_{\alpha\beta}}{2} \right) p_{j-1,\beta} + \text{H.c.} \right] \tag{6}$$

describes a different type of process, characterized by a nonlocal hopping accompanied by a spin flip.

We have studied the ground-state properties of H by means of DMRG. In our implementation we have kept $m = 800$ states and we have swept the finite-size procedure 12 times, which allowed us to achieve truncation errors in the density matrix of the order of 10^{-12} at best, and 10^{-8} in the worst situation. The DMRG method has been used previously to describe the standard 1D Kondo lattice model at half filling [24–28], where a topologically trivial, fully gapped ground state was obtained. For the p-KHM, where a topological insulator ground state was predicted [20,33], there are no DMRG studies to the best of our knowledge. Intuitively, we expect that the charge and spin gaps in this model vanish in the limit $J_K \to 0$, as the Hamiltonians H_1 and H_2 are separately gapless in the thermodynamic limit. According to the bosonization analysis in the limit of small J_K, both gaps are favored when the velocities of the gapless spinon excitations described by H_1 and H_2 coincide. Intuitively, the term H_K becomes more effective to couple the spin degrees of freedom in H_1 and H_2 when they fluctuate coherently (i.e., same spinon velocities). The spinon velocity in the conduction band is equal to the tight-binding Fermi velocity $v_1 = v_F = 2t$, and in the Heisenberg chain is $v_2 = \pi J_H/2$ [42,43], and therefore we conclude that the optimal situation in order to maximize the effect of H_K corresponds to $J_H = 4t/\pi \approx 1.27\ t$, which we choose in all our subsequent calculations. In what follows, we characterize the ground state by analyzing the charge and spin gaps, the string order parameter, and spin profile along the chain.

III. CHARGE GAP

Spin-flip scattering generated upon increasing J_K induces gapped charge and spin excitations in the system at half filling [20,33]. Although these gaps are not direct evidence of the topological nature of the ground state, their study is important to characterize the p-KHM insulating phase and to test the predictions of bosonization. The hidden SU(2) charge pseudospin symmetry of the model at half filling allows us to compute the energy of the first charge excitation of a system with N electrons as the ground-state energy of a system with $N+2$ electrons [26,28]. Therefore, we can compute the charge gap of a L-supersite system as $\Delta_c(L) = E_0^{M^z=0}(N=L+2) - E_0^{M^z=0}(N=L)$. Here, a "supersite" j refers to the combination of a spin $\mathbf{S}_j$ and the fermionic site in each rung, therefore spanning an eight-dimensional local basis. M^z is the z projection of the total spin in the system, computed as $M^z = \sum_{j=1}^{L} \langle T_j^z \rangle$, where $\mathbf{T}_j \equiv \mathbf{S}_j + \mathbf{s}_j$. Finally, $E_0^{M^z}(N)$ is the ground-state energy of a system with N electrons in the conduction band, and projection M^z.

Previous results on the standard 1D Kondo lattice, without direct exchange J_H between the magnetic ions, predicted a linear dependence $\Delta_c \propto J_K$ [21,28]. However, in a recent study, based in bosonization [33], it has been shown that in the presence of a direct exchange J_H, the charge gap appears as a second-order process in the Kondo coupling. This can be physically understood noting that, in the presence of a large J_H, the action of the perturbation J_K generates a spin excitation (a "spinon") in the Heisenberg chain and an electronic excitation in the conduction band. Using, for instance, second-order perturbation theory in J_K, one can see that two of these electronic excitations become mediated by a spinon excitation in the Heisenberg chain, and effectively generate a four-fermion interaction term in the conduction band. This process is similar to the phonon-mediated electron-electron interaction in BCS theory, which appears at second order in the electron-phonon interaction. In our case, however, the effective interaction which appears upon integrating out the "spinon" field turns out to be repulsive instead of attractive. The net result, is the emergence of an effective repulsion term U, similar to the one in the Hubbard chain model. Therefore, in the half-filled p-KHM, a Mott gap $\Delta_c \propto J_K^2/J_H$ opens in the system. Note that in absence of J_H, as in Refs. [21] and [28], this process cannot exist as the spins are not directly connected, and there are no spinons.

We compare this prediction against DMRG results. In Fig. 2 we show the charge gap as a function of J_K. The system presents important finite-size effects in the limit of small J_K, and we therefore analyze our results with the scaling law $\Delta_c(L) \approx \Delta_c(\infty) + \beta_c L^{-2}$ in the case of large J_K ($J_K/t > 0.3$) [25,28], whereas in the regime of smaller $J_K/t < 0.3$ the fits improve with the scaling law $\Delta_c(L) \approx \sqrt{\Delta_c^2(\infty) + \beta_c L^{-2}}$ (see inset in Fig. 2). The scaling was conducting using supersite lattices of sizes L=40, 60, 80, 100, and 120. This fitting procedure allows us to extract $\Delta_c(\infty)$, the value of the charge gap in the thermodynamic limit, as a function of J_K (see Fig. 2). The solid (red) line is a quadratic law $\Delta_c(\infty) = \alpha_c J_K^2$ which fits the data reasonably well at small J_K, confirming the dependence predicted by bosonization [33].

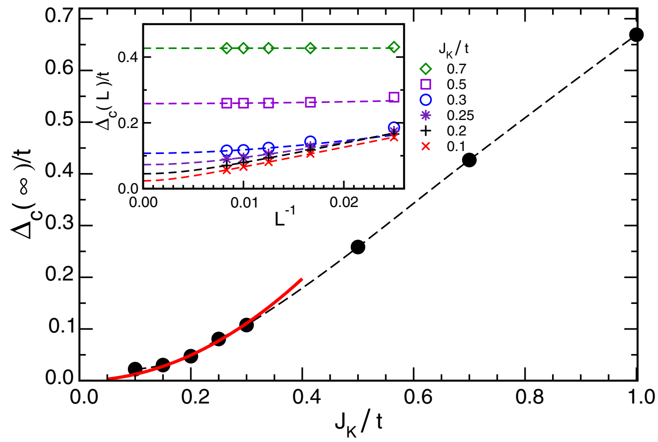

FIG. 2. (Color online) Charge gap in the thermodynamical limit $\Delta_c(\infty)$ (shown as black circles) vs J_K, obtained after finite-size scaling (see inset). The solid (red) line is a fit $\Delta_c(\infty) = \alpha_c J_K^2$, valid for small J_K, based on the bosonization analysis of Ref. [33]. Dashed lines are a guide to the eye. Inset: Finite-size scaling using the scaling laws $\Delta_c(L) \approx \Delta_c(\infty) + \beta_c L^{-2}$ for $J_K/t > 0.3$ [25,28], and $\Delta_c(L) \approx \sqrt{\Delta_c^2(\infty) + \beta_c L^{-2}}$ for $J_K/t < 0.3$.

IV. SPIN GAP AND SPIN-1/2 END STATES

We now focus on the spin degrees of freedom, where the p-KHM has the most interesting properties. Intuitively, the physics of the problem can be simply understood: the antiferromagnetic Kondo exchange along the diagonal rungs, combined with the antiferromagnetic spin correlations along the legs, effectively forces the spins to align *ferromagnetically* across the rungs, even in the absence of a direct coupling [33]. This situation favors the formation of a local triplet in each supersite, and the system mimics the properties of the spin-1 Heisenberg chain [44] or the ferromagnetic Kondo lattice model [24,45], which are examples of systems realizing an insulating Haldane ground state. A hallmark of this phase is the presence of two topologically protected spin-1/2 magnetic states at the ends of the chain (i.e., $|\uparrow\rangle_L \otimes |\uparrow\rangle_R$, $|\uparrow\rangle_L \otimes |\downarrow\rangle_R$, $|\downarrow\rangle_L \otimes |\uparrow\rangle_R$, and $|\downarrow\rangle_L \otimes |\downarrow\rangle_R$), which arrange into triplet and singlet linear combinations which are degenerate in the thermodynamical limit $L \to \infty$. As a result, the first spin-excitation gap $\Delta_s^{(1,0)}(L) \equiv E_0^{M^z=1}(N=L) - E_0^{M^z=0}(N=L)$, tends to zero in that case. For a finite-L chain, however, the overlap of the end-states wave functions removes this degeneracy exponentially as $\Delta_s^{(1,0)}(L) \propto e^{-L/\xi}$, where $\xi \propto J_K^{-1}$ is the localization length for the magnetic end states, and the ground state for N even (odd) corresponds to the singlet $S=0$ (triplet $S=1$) combination [41]. In our case, at small J_K the localization length ξ becomes of the order of the system size ($\xi \sim L$), and it was not possible to obtain a conclusive scaling behavior for $\Delta_s^{(1,0)}$, even for the largest systems we have simulated ($L=120$).

On the other hand, the gap $\Delta_s^{(2,0)}$ (same definition as above changing $M^z = 1 \to M^z = 2$) can be identified with

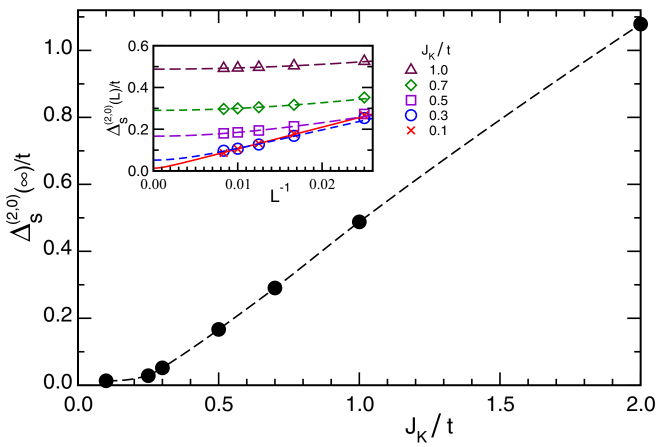

FIG. 3. (Color online) Extrapolated spin gap $\Delta_s^{(2,0)}(\infty)$ (corresponding to the Haldane gap), as a function of J_K, obtained after a finite-size scaling analysis (see inset). Dashed lines are a guide to the eye. Inset: Finite-size scaling using the scaling law $\Delta_s(L) \approx \sqrt{\Delta_s^2(\infty) + \beta_s L^{-2}}$.

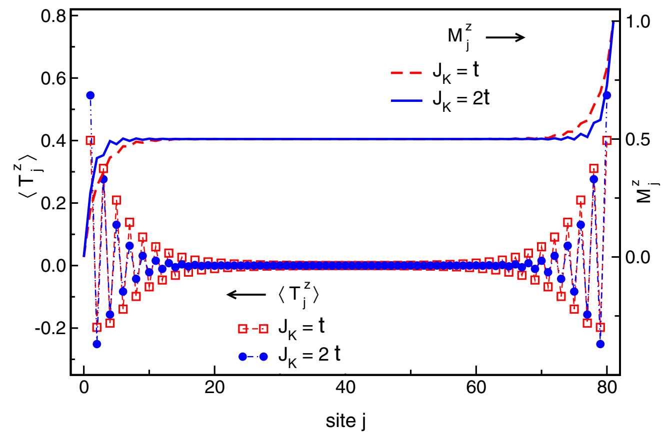

FIG. 4. (Color online) Spatial profile of $\langle T_j^z \rangle = \langle \psi_g^{M^z=1} | T_j^z | \psi_g^{M^z=1} \rangle$, i.e., the z component of the spin in the supersite j (left y axis), computed with the ground state of the subspace with total $M^z = 1$ for $L = 80$. We also show the accumulated magnetization up to a given site j: $M_j{}^z \equiv \sum_{i=1}^{j} \langle T_i^z \rangle$ (right y axis). The presence of the topologically protected spin-1/2 states at the ends of the chain is clearly seen.

the Haldane gap of the system, and physically involves spin excitations which live in the bulk (see Fig. 3). In this case, the scaling analysis is simpler as it is free from edge effects, and we have used the scaling law $\Delta_s(L) \approx \sqrt{\Delta_s^2(\infty) + \beta_s L^{-2}}$ for all values of J_K (see inset in Fig. 3). The values of $\Delta_s(\infty)$ are shown in Fig. 3. In contrast to the case of the charge gap, here the analytic dependence of $\Delta_s(\infty)$ on the parameter J_K is technically more challenging to obtain within the bosonization formalism, and is beyond the scope of this work. Nevertheless, our numerical results suggest a power-law dependence $\Delta_s(\infty) \propto J_K^{\nu}$, with exponent $\nu \gtrsim 2$ in the limit of small J_K.

We next investigate the presence of topologically protected spin-1/2 end states which, as mentioned before, is a crucial feature of the open Haldane chain. In Fig. 4 we show a spatial profile of the z projection of $\mathbf{T}_j$, i.e., $\langle T_j^z \rangle = \langle \psi_g^{M^z=1} | T_j^z | \psi_g^{M^z=1} \rangle$, where $| \psi_g^{M^z=1} \rangle$ is the ground state with total spin $M^z = 1$, for $J_K/t = 1$ (red squares) and $J_K/t = 2$ (blue circles). For these large values of J_K (which are beyond the validity of the bosonization analysis [33]) the end states are clearly visible and show a small localization length ξ, a fact that prevents them from overlapping, producing negligible finite-size effects. The accumulated magnetization ($M_j^z = \sum_{i=1}^{j} \langle T_i^z \rangle$) up to a site j is also shown in solid lines in Fig. 4 (the red dashed line corresponds to $J_K/t = 1$ and the solid blue line corresponds to $J_K/t = 2$), and corresponds to the right y axis. It can be seen that the accumulated spin at each end is 1/2, corresponding to the configuration where the topological spin-1/2 end states is $|\psi_g^{M^z=1}\rangle \propto |\uparrow\rangle_L \otimes |\uparrow\rangle_R$ [34,35].

V. STRING ORDER PARAMETER

The most fundamental signature of the Haldane phase is, however, the emergence of a finite string order parameter [46], a quantity deeply connected to a broken hidden $Z_2 \times Z_2$ symmetry [36]. This quantity is a smoking gun for the presence of the Haldane phase, and therefore is the most important for our present purposes. Using the above definition of $\mathbf{T}_j$, the string order parameter is defined as

$$\mathcal{O}^{\alpha}_{\text{string}}(l-m) \equiv -\left\langle T_l^{\alpha} e^{i\pi \sum_{l<j<m} T_j^{\alpha}} T_m^{\alpha} \right\rangle. \tag{7}$$

Due to the SU(2) spin-symmetry of the model, it is enough to calculate the computationally simpler component $\alpha = z$. We have computed $\mathcal{O}^{z}_{\text{string}}(l-m)$ taking the sites l and m symmetrically about the center of the system in order to minimize the effect of the edges. Note in the inset of Fig. 5 that $\mathcal{O}^{z}_{\text{string}}(d)$ converges rapidly as a function of the distance $d = |l-m|$ to the 1D-bulk value $\mathcal{O}^{z,\text{bulk}}_{\text{string}}$. In the main Fig. 5 we show $\mathcal{O}^{z,\text{bulk}}_{\text{string}}$ vs J_K, which remains finite throughout the whole studied regime. This indicates the presence of a Haldane phase even beyond the regime of small J_K where the bosonization analysis in Ref. [33] is valid. This result, together with the

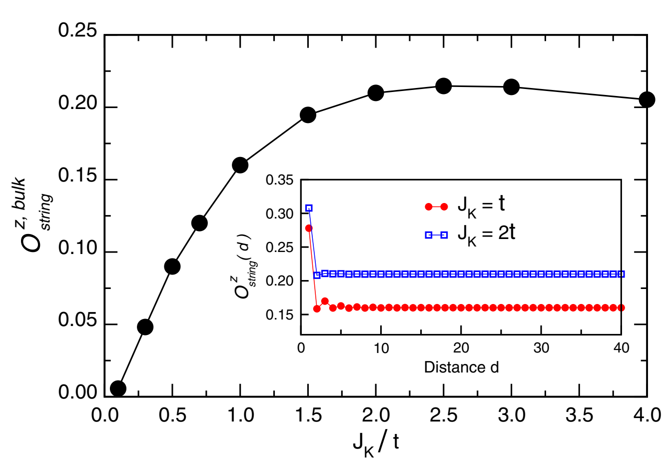

FIG. 5. (Color online) String order parameter $\mathcal{O}^{z,\text{bulk}}_{\text{string}}$ vs J_K. Throughout the whole studied regime, $\mathcal{O}^{z,\text{bulk}}_{\text{string}}$ remains finite, indicating the presence of a Haldane-insulating phase. Inset: Spatial dependence of $\mathcal{O}^{z}_{\text{string}}(d)$ vs the distance $d = |l-m|$, where l and m have been taken symmetrically about the center of the chain.

confirmation of the presence of spin-1/2 end states, are the most important results of this paper, as they provide conclusive evidence that the p-KHM realizes a Haldane phase.

VI. EXPERIMENTAL REALIZATION IN OPTICAL LATTICES

Optical lattices with higher orbital bands have recently attracted a lot of experimental [47–49] and theoretical [50–52] interest due to their ability to realize novel topological phases of matter. In this section, we discuss how p-band optical lattices could be used to realize the p-KHM. To that end, we can think of the ladder depicted in Fig. 1(c) as the quasi-1D limit of the optical lattice potential

$$V(x,y) = V_x \sin^2(kx) + V_1 \sin^2(ky) + V_2 \sin^2\left(2ky + \frac{\phi}{2}\right), \tag{8}$$

which has a double-well structure in the $\hat{y}$ direction. In particular when $\{V_1, V_2\} \gg V_x$, there is a large potential barrier between the wells along the $\hat{y}$ direction, and at low energies the two-dimensional system effectively becomes a collection of weakly coupled two-leg ladders [see Fig. 1(c)]. The relative well depth of the two legs can be controlled by the ratio V_2/V_1 and by the relative phase ϕ. Furthermore, we assume that the optical lattice is loaded with a balanced mixture of two-component Fermi atoms (e.g., ^{6}Li or ^{40}K), simulating spin-1/2 fermions.

We now focus on a situation where the p-orbital level in the right leg in Fig. 1(b) has approximately the same energy as the s-orbital level in the left leg. Moreover, we assume that the Fermi energy and the temperature are such that no other higher orbitals are occupied. In this situation, the dynamics of the fermions in the p-orbital leg is dictated by our tight-binding Hamiltonian H_1 in Eq. (1), which arises after considering tunneling processes between nearest-neighbor sites $t \propto \langle p_j | V_x \sin^2(kx) | p_{j+1}\rangle$ along the $\hat{x}$ direction.

Similarly, the s-orbital leg can be described by the Hubbard model

$$H_{\text{Hubbard}} = -t' \sum_{\langle ij\rangle,\sigma}^{N} (s^\dagger_{i,\sigma} s_{j,\sigma} + \text{H.c.}) + U \sum_{i}^{N} \left(n^{(s)}_{i,\uparrow} - \frac{1}{2}\right)\left(n^{(s)}_{i,\downarrow} - \frac{1}{2}\right), \tag{9}$$

where $s^\dagger_{j,\sigma}$ is a creation operator of a fermion with spin σ at the s-orbital site j, and $n^{(s)}_{j,\sigma} = s^\dagger_{j,\sigma} s_{j,\sigma}$ is the fermion occupation. Here $t' \propto \langle s_j | V_x \sin^2(kx) | s_{j+1}\rangle$ is the hopping matrix element, and U is an on-site Coulomb interaction, assumed to arise due to a Feschbach resonance induced with an external magnetic field. In the limit $U \gg t'$, and when $n^{(s)}_{j,\sigma} = 1$ (i.e., half filling), the Hubbard model Hamiltonian (9) maps onto the Heisenberg chain H_2 model Eq. (2) [53,54].

We now consider a small tunneling between s and p orbitals in different legs, which would give rise to a microscopic single-particle hopping Hamiltonian $H_{\text{s-p}}$ connecting H_1 and H_{Hubbard}. However, due to the different parities of the s and p orbitals along the x axis, the matrix element connecting sites on the same rung vanishes (i.e., the orbitals are orthogonal $\langle s_j | p_j\rangle = 0$). Then, the leading contribution to $H_{\text{s-p}}$ corresponds to the matrix element V coupling s and p orbitals along *diagonal* rungs, i.e.,

$$H_{\text{s-p}} = V \sum_{j,\sigma} s^\dagger_{j,\sigma}(p_{j+1,\sigma} - p_{j-1,\sigma}) + \text{H.c.} \tag{10}$$

Note the crucial sign inside the parentheses, which appears as a direct consequence of the p-wave nature of the conduction p-band states.

We now claim that tuning both the s and p bands at (or sufficiently close to) half filling, and in the strong-coupling regime $U' \gg \{t', V\}$ (two conditions consistent with the previous assumptions due to the high degree of tunability of optical lattices), the microscopic Hamiltonian of the interacting ladder

$$H' = H_1 + H_{\text{Hubbard}} + H_{\text{s-p}} \tag{11}$$

effectively maps at low energies onto the p-KHM, providing a physical system where the results of this work could be experimentally tested. In addition, it provides a physical justification for the unusual p-wave Kondo interaction Eq. (3). This equivalence, outlined below, can be rigorously shown by the means of a canonical (i.e., a generalized Schrieffer-Wolff) transformation.

The basic idea consists of introducing an operator $\mathcal{T} \equiv e^{i\mathcal{S}}$, where $\mathcal{S} = \mathcal{S}(t', V)$ is chosen so as to eliminate the first-order contributions in t' and V. The procedure is standard and here we only outline the main steps (see the Appendix for details). Assuming $t', V \ll U$, we can expand the exponential in $\mathcal{T}$ and truncate the series at second order in (t'/U) and (V/U), therefore obtaining

$$H = \mathcal{T}^\dagger H' \mathcal{T} \approx H' + i[\mathcal{S}, H'] + \frac{i^2}{2!}[\mathcal{S},[\mathcal{S},H']]. \tag{12}$$

We choose the transformation as

$$\mathcal{S} = -i[(H^+_{t'} - H^-_{t'}) + 2(H^+_{\text{s-p}} - H^-_{\text{s-p}})]/U', \tag{13}$$

with

$$H^+_{t'} = -t' \sum_{\langle ij\rangle,\sigma}^{N} n^{(s)}_{i,\bar{\sigma}} s^\dagger_{i,\sigma} s_{j,\sigma}\left(1 - n^{(s)}_{j,\bar{\sigma}}\right), \tag{14}$$

and

$$H^+_{\text{s-p}} = V \sum_{i,\sigma} \left[n^{(s)}_{i,\bar{\sigma}} s^\dagger_{i,\sigma}(p_{i+1,\sigma} - p_{i-1,\sigma}) s_{i,\sigma}\left(1 - n^{(s)}_{i,\bar{\sigma}}\right)\right] \tag{15}$$

(with $\langle ij\rangle$ indicating nearest neighbors), and where $H^-_{t'} = (H^+_{t'})^\dagger$ and $H^-_{\text{s-p}} = (H^+_{\text{s-p}})^\dagger$. We can check that the first-order contributions cancel, and therefore

$$H_2 = -\frac{1}{U}\mathcal{P}(H^-_{t} H^+_{t})\mathcal{P}, \tag{16}$$

and

$$H_K = -\frac{2}{U}\mathcal{P}(H^-_{\text{s-p}} H^+_{\text{s-p}})\mathcal{P}, \tag{17}$$

where $\mathcal{P}$ is the projector onto the lowest subspace of H_{Hubbard} (see the Appendix). The connection between the Hamiltonian (11) and the p-KHM is completed identifying the parameters as $J_H \equiv 4t'^2/U$ and $J_K \equiv 8V^2/U$. We note that this proposal is different from other theoretical proposals to simulate the standard Kondo lattice model in 1D optical lattices [55,56].

VII. CONCLUSIONS

We have studied the p-KHM, a theoretical "toy model" introduced to describe a 1DTKI. By means of DMRG, we have calculated various quantities characterizing the ground state at half filling. We have shown strong numerical evidence (based on the analysis of the charge and spin gaps, the spin profile, and the string order parameter) that the p-KHM realizes a Haldane phase at low temperatures. Our results indicate that the topological properties of this model fall beyond the scope of the noninteracting topological classification [7–9], which is unable to reveal the true topological structure of the ground state. Finally, we have proposed that the unusual p-wave Kondo interaction could be physically realized in experiments with ultracold Fermi gases loaded in p-band optical lattices.

ACKNOWLEDGMENTS

We are grateful to L. O. Manuel for useful discussions and for revising this manuscript. The authors acknowledge support from CONICET (Argentina), PIP 11220120100389CO.

APPENDIX: DERIVATION OF THE p-KHM BY A CANONICAL TRANSFORMATION

In this Appendix we provide a derivation of the p-KHM Hamiltonian H in the main text by the means of a canonical transformation. To that end, we start from the microscopic Hamiltonian H', consisting of a fermionic Hubbard ladder with s and p orbitals along the legs, and depicted in Fig. 1(b) in the main text:

$$H' = H_{\text{Hubbard}} + H_{\text{s-p}} + H_1, \tag{A1}$$

$$H_{\text{Hubbard}} = -t' \sum_{j,\sigma}^{L-1} (s^{\dagger}_{j,\sigma} s_{j+1,\sigma} + \text{H.c.}) \tag{A2}$$

$$+ U \sum_{j=1}^{L} \left(n^{(s)}_{j,\uparrow} - \frac{1}{2} \right)\left(n^{(s)}_{j,\downarrow} - \frac{1}{2} \right), \tag{A3}$$

$$H_1 = -t \sum_{j=1,\sigma}^{L-1} (p^{\dagger}_{j,\sigma} p_{j+1,\sigma} + \text{H.c.}), \tag{A4}$$

$$H_{\text{s-p}} = V \sum_{j,\sigma} s^{\dagger}_{j,\sigma} (p_{j+1,\sigma} - p_{j-1,\sigma}) + \text{H.c.} \tag{A5}$$

Note that the system has electron-hole symmetry. Here, $s^{\dagger}_{j,\sigma}$ creates a fermion with spin projection σ at site j in the Hubbard leg and $n^{(s)}_{j\sigma} \equiv s^{\dagger}_{j,\sigma} s_{j,\sigma}$ is the corresponding fermion-number operator. The operator $p^{\dagger}_{j,\sigma}$ creates a fermion with spin σ at site j in the p-orbital conduction band, represented by a simple tight-binding model H_1. The term $H_{\text{s-p}}$ couples the two fermionic legs, and due to the symmetry properties of the s and p orbitals, the direct hopping across the rungs is zero. Therefore, the most important hopping process occurs between a fermion $s_{j,\sigma}$ and the linear superposition with p-wave symmetry $\propto (p_{j+1,\sigma} - p_{j-1,\sigma})$ in the conduction band.

The idea is to derive an effective low-energy model in the limit $U \gg \{t', V\}$. To that end, we split the Hamiltonian H' into

$$H' = H_{t'} + H_{\text{s-p}} + H_U + H_1, \tag{A6}$$

where

$$H_{t'} = -t' \sum_{\langle ij \rangle,\sigma}^{L} (s^{\dagger}_{i,\sigma} s_{j,\sigma} + \text{H.c.}), \tag{A7}$$

$$H_U = U \sum_{j}^{L} \left(n_{j,\uparrow} - \frac{1}{2} \right)\left(n_{j,\downarrow} - \frac{1}{2} \right). \tag{A8}$$

The first two terms in (A6) will be considered as perturbations to H_U, in the regime $\{t', V\} \ll U$.

We now start from the atomic limit in the Hubbard leg, i.e., $t' = V = 0$, and identify the atomic singly occupied states $|\sigma_j\rangle = s^{\dagger}_{j,\sigma}|0\rangle$ ($\sigma = \uparrow,\downarrow$) as forming the lowest-energy subspace at site j, while the $|0_j\rangle$ (empty) and $|d_j\rangle = s^{\dagger}_{j,\uparrow} s^{\dagger}_{j,\downarrow}|0\rangle$ (doubly occupied) form the excited subspace. We now introduce projectors onto each of the four atomic states:

$$\mathcal{P}_{j,0} = \left(1 - n^{(s)}_{j,\uparrow}\right)\left(1 - n^{(s)}_{j,\downarrow}\right), \tag{A9}$$

$$\mathcal{P}_{j,d} = n^{(s)}_{j,\uparrow} n^{(s)}_{j,\downarrow}, \tag{A10}$$

$$\mathcal{P}_{j,\uparrow} = n^{(s)}_{j,\uparrow}\left(1 - n^{(s)}_{j,\downarrow}\right), \tag{A11}$$

$$\mathcal{P}_{j,\downarrow} = n^{(s)}_{j,\downarrow}\left(1 - n^{(s)}_{j,\uparrow}\right). \tag{A12}$$

Note that while all projectors commute with H_U, the kinetic terms $H_{t'}$ and $H_{\text{s-p}}$ cause transitions among subspaces. Using that $\mathbf{1}_j = \sum_{\alpha} \mathcal{P}_{j,\alpha}$, we can write the kinetic terms as $H_{t'} = (\sum_{i,\alpha} \mathcal{P}_{i,\alpha}) H_{t'} (\sum_{j,\beta} \mathcal{P}_{j,\beta}) = H^{+}_{t'} + H^{-}_{t'} + H^{0}_{t'}$, and $H_{\text{s-p}} = (\sum_{i,\alpha} \mathcal{P}_{i,\alpha}) H_{\text{s-p}} (\sum_{j,\beta} \mathcal{P}_{j,\beta}) = H^{+}_{\text{s-p}} + H^{-}_{\text{s-p}} + H^{0}_{\text{s-p}}$, where

$$H^{+}_{t'} = -t' \sum_{\langle ij \rangle,\sigma}^{N} \left[n^{(s)}_{i,\bar{\sigma}} s^{\dagger}_{i,\sigma} s_{j,\sigma}\left(1 - n^{(s)}_{j,\bar{\sigma}}\right) + n^{(s)}_{j,\bar{\sigma}} s^{\dagger}_{j,\sigma} s_{i,\sigma}\left(1 - n^{(s)}_{i,\bar{\sigma}}\right)\right], \tag{A13}$$

$$H^{-}_{t'} = -t' \sum_{\langle ij \rangle,\sigma}^{N} \left[\left(1 - n^{(s)}_{j,\bar{\sigma}}\right) s^{\dagger}_{j,\sigma} s_{i,\sigma} n^{(s)}_{i,\bar{\sigma}} + \left(1 - n^{(s)}_{i,\bar{\sigma}}\right) s^{\dagger}_{i,\sigma} s_{j,\sigma} n^{(s)}_{j,\bar{\sigma}}\right], \tag{A14}$$

$$H^{+}_{\text{s-p}} = V \sum_{i,\sigma} \left[n^{(s)}_{i,\bar{\sigma}} s^{\dagger}_{i,\sigma} (p_{i+1,\sigma} - p_{i-1,\sigma}) + (p^{\dagger}_{i+1,\sigma} - p^{\dagger}_{i-1,\sigma}) s_{i,\sigma}\left(1 - n^{(s)}_{i,\bar{\sigma}}\right)\right], \tag{A15}$$

$$H^{-}_{\text{s-p}} = V \sum_{i,\sigma} \left[(p^{\dagger}_{i+1,\sigma} - p^{\dagger}_{i-1,\sigma}) s_{i,\sigma} n^{(s)}_{i,\bar{\sigma}} + \left(1 - n^{(s)}_{i,\bar{\sigma}}\right) s^{\dagger}_{i,\sigma} (p_{i+1,\sigma} - p_{i-1,\sigma})\right]. \tag{A16}$$

Physically, the terms with supraindex "+" produce transitions from the lowest subspace to the excited subspace, while those with "−" restore excited states to the lowest subspace. On the other hand, the terms labeled with "0" do not change the subspace, and since we assume a half-filled conduction band, they will identically vanish and it is not necessary to write them explicitly here. We now note the following important relations:

$$H_{t'}^{-} = (H_{t'}^{+})^{\dagger}, \tag{A17}$$

$$H_{\text{s-p}}^{-} = (H_{\text{s-p}}^{+})^{\dagger}, \tag{A18}$$

which will be useful in what follows.

We now introduce a canonical transformation in Eq. (A1), such that in the transformed representation we simultaneously get rid of the terms at first order in t' and V:

$$H = e^{i\mathcal{S}} H' e^{-i\mathcal{S}}. \tag{A19}$$

$$= H' + i[\mathcal{S},H'] + \frac{i^2}{2!}[\mathcal{S},[\mathcal{S},H']] + \dots. \tag{A20}$$

We want to choose $\mathcal{S}$ in such a way that H does not connect different Hubbard subbands. Note that this cannot be achieved at infinite order in the expansion in powers of $\mathcal{S}$ in Eq. (A20), but we will be content if we can eliminate the contributions at order $\mathcal{O}(t')$ and $\mathcal{O}(V)$ that mix the subbands. We now write the expansion in Eq. (A20) in the more suggestive form

$$H = H_{t'}^{+} + H_{t'}^{-} + H_{\text{s-p}}^{+} + H_{\text{s-p}}^{-} + i[\mathcal{S},H_U] \tag{A21}$$

$$+ H_1 + H_U + i[\mathcal{S},H_{t'}^{+} + H_{t'}^{-}] + i[\mathcal{S},H_{\text{s-p}}^{+} + H_{\text{s-p}}^{-}]$$

$$+ \frac{i^2}{2!}[\mathcal{S},[\mathcal{S},H_U]] \tag{A22}$$

$$+ (\text{other less important terms}) \tag{A23}$$

We will require that the first line (A21) in the above equation vanishes. It is then clear that $\mathcal{S}$ must be $\mathcal{O}(t'/U) \sim \mathcal{O}(V/U)$. Using the following results

$$\left[n_{i,\bar{\sigma}}^{(s)} s_{i,\sigma}^{\dagger} s_{j,\sigma}\left(1 - n_{j,\bar{\sigma}}^{(s)}\right), \left(n_{i,\sigma}^{(s)} - t\tfrac{1}{2}\right)\left(n_{i,\bar{\sigma}}^{(s)} - \tfrac{1}{2}\right)\right] = \left[n_{i,\bar{\sigma}}^{(s)} s_{i,\sigma}^{\dagger} s_{j,\sigma}\left(1 - n_{j,\bar{\sigma}}^{(s)}\right), \left(n_{j,\sigma}^{(s)} - \tfrac{1}{2}\right)\left(n_{j,\bar{\sigma}}^{(s)} - \tfrac{1}{2}\right)\right] \tag{A24}$$

$$= -\tfrac{1}{2} n_{i,\bar{\sigma}}^{(s)} s_{i,\sigma}^{\dagger} s_{j,\sigma}\left(1 - n_{j,\bar{\sigma}}^{(s)}\right), \tag{A25}$$

$$\left[n_{i,\bar{\sigma}}^{(s)} s_{i,\sigma}^{\dagger}(p_{i+1,\sigma} - p_{i-1,\sigma}), \left(n_{i,\sigma}^{(s)} - \tfrac{1}{2}\right)\left(n_{i,\bar{\sigma}}^{(s)} - \tfrac{1}{2}\right)\right] = -\tfrac{1}{2} n_{i,\bar{\sigma}}^{(s)} s_{i,\sigma}^{\dagger}(p_{i+1,\sigma} - p_{i-1,\sigma}), \tag{A26}$$

$$\left[(p_{i+1,\sigma}^{\dagger} - p_{i-1,\sigma}^{\dagger}) s_{i,\sigma}\left(1 - n_{i,\bar{\sigma}}^{(s)}\right), \left(n_{i,\sigma}^{(s)} - \tfrac{1}{2}\right)\left(n_{i,\bar{\sigma}}^{(s)} - \tfrac{1}{2}\right)\right] = -\tfrac{1}{2}(p_{i+1,\sigma}^{\dagger} - p_{i-1,\sigma}^{\dagger}) s_{i,\sigma}\left(1 - n_{i,\bar{\sigma}}^{(s)}\right), \tag{A27}$$

it is easy to check that

$$[H_{t'}^{\pm}, H_U] = \mp U H_{t'}^{\pm}, \tag{A28}$$

$$[H_{\text{s-p}}^{\pm}, H_U] = \mp \frac{U}{2} H_{\text{s-p}}^{\pm}. \tag{A29}$$

Then, it follows that the choice

$$\mathcal{S} = -\frac{i}{U}(H_{t'}^{+} - H_{t'}^{-}) - \frac{2i}{U}(H_{\text{s-p}}^{+} - H_{\text{s-p}}^{-}) \tag{A30}$$

exactly cancels line (A21).

The relevant part of the Hamiltonian at low energies is then obtained projecting H onto the lowest Hubbard subband. This is formally done applying the projector $\mathcal{P} = \sum_i (\mathcal{P}_{i,\uparrow} + \mathcal{P}_{i,\downarrow})$, which eliminates certain terms in Eqs. (A22) and (A23). The resulting effective Hamiltonian at lowest order in t/U and V/U is therefore

$$H = H_1 + \mathcal{P}\Big\{H_U + i[\mathcal{S},H_{t'}^{+} + H_{t'}^{-}] + i[\mathcal{S},H_{\text{s-p}}^{+} + H_{\text{s-p}}^{-}]$$

$$+ \frac{i^2}{2!}[\mathcal{S},[\mathcal{S},H_U]]\Big\}\mathcal{P}$$

$$= H_1 + H_U - \frac{1}{U}\mathcal{P}(H_{t'}^{-} H_{t'}^{+})\mathcal{P} - \frac{2}{U}\mathcal{P}(H_{\text{s-p}}^{-} H_{\text{s-p}}^{+})\mathcal{P}. \tag{A31}$$

We now replace the expressions for $H_{t'}^{\pm}$ and $H_{\text{s-p}}^{\pm}$ [Eqs. (A13)–(A16)] into the above equation and obtain

$$\mathcal{P}\left(H_{t'}^{-} H_{t'}^{+}\right)\mathcal{P} = (t')^2 \sum_{i,\sigma}^{N} [\mathcal{P}_{i,\bar{\sigma}}\mathcal{P}_{i+1,\sigma} + \mathcal{P}_{i,\sigma}\mathcal{P}_{i+1,\bar{\sigma}} - s_{i+1,\sigma}^{\dagger} s_{i+1,\bar{\sigma}} s_{i,\bar{\sigma}}^{\dagger} s_{i,\sigma} - s_{i+1,\bar{\sigma}}^{\dagger} s_{i+1,\sigma} s_{i,\sigma}^{\dagger} s_{i,\bar{\sigma}}], \tag{A32}$$

$$\mathcal{P}(H_{\text{s-p}}^{-} H_{\text{s-p}}^{+})\mathcal{P} = 2V^2 \sum_{i,\sigma} n_{i,\sigma}^{(s)} - V^2 \sum_{i,\sigma} \big[(n_{i,\sigma}^{(s)} - n_{i,\bar{\sigma}}^{(s)})(p_{i+1,\sigma}^{\dagger} - p_{i-1,\sigma}^{\dagger})(p_{i+1,\sigma} - p_{i-1,\sigma})$$

$$+ s_{i,\bar{\sigma}}^{\dagger} s_{i,\sigma}(p_{i+1,\sigma}^{\dagger} - p_{i-1,\sigma}^{\dagger})(p_{i+1,\bar{\sigma}} - p_{i-1,\bar{\sigma}}) + s_{i,\sigma}^{\dagger} s_{i,\bar{\sigma}}(p_{i+1,\bar{\sigma}}^{\dagger} - p_{i-1,\bar{\sigma}}^{\dagger})(p_{i+1,\sigma} - p_{i-1,\sigma})\big]. \tag{A33}$$

Using that $\mathcal{P}_{i,\uparrow}\mathcal{P}_{i+1,\downarrow} + \mathcal{P}_{i,\downarrow}\mathcal{P}_{i+1,\uparrow} = -2S_i^z S_{i+1}^z + n_i^{(s)} n_{i+1}^{(s)}/2$, and the Schwinger-fermion representation

$$S_i^z = \frac{n_{i,\uparrow}^{(s)} - n_{i,\downarrow}^{(s)}}{2}, \tag{A34}$$

$$S_i^{+} = s_{i,\uparrow}^{\dagger} s_{i,\downarrow}, \tag{A35}$$

$$S_i^{-} = s_{i,\downarrow}^{\dagger} s_{i,\uparrow} \tag{A36}$$

is a faithful representation of a spin-1/2 operator, we can write the effective Hamiltonian as

$$H = H_U + H_1 + \frac{4(t')^2}{U}\sum_i^N \left[S_i^z S_{i+1}^z + \frac{S_{i+1}^+ S_i^- + S_{i+1}^- S_i^+}{2} - \frac{1}{4}\right] + \frac{8V^2}{U}\sum_i S_i^z \frac{(p_{i+1,\uparrow}^\dagger - p_{i-1,\uparrow}^\dagger)(p_{i+1,\uparrow} - p_{i-1,\uparrow}) - (p_{i+1,\downarrow}^\dagger - p_{i-1,\downarrow}^\dagger)(p_{i+1,\downarrow} - p_{i-1,\downarrow})}{2} + \frac{8V^2}{U}\sum_i \left[\frac{S_i^+(p_{i+1,\downarrow}^\dagger - p_{i-1,\downarrow}^\dagger)(p_{i+1,\uparrow} - p_{i-1,\uparrow})}{2} + \frac{S_i^-(p_{i+1,\uparrow}^\dagger - p_{i-1,\uparrow}^\dagger)(p_{i+1,\downarrow} - p_{i-1,\downarrow})}{2}\right], \tag{A37}$$

where we have neglected the constant $\frac{2V^2}{U}\sum_{i,\sigma} n_{i,\sigma}^{(s)}$. Defining the effective parameters

$$J_H \equiv \frac{4(t')^2}{U}, \tag{A38}$$

$$J_K \equiv \frac{8V^2}{U}, \tag{A39}$$

we note that this Hamiltonian corresponds to the p-KHM considered by Alexandrov and Coleman [20].

[1] B. A. Bernevig, T. L. Hughes, and S.-C. Zhang, Science **314**, 1757 (2006).
[2] L. Fu and C. L. Kane, Phys. Rev. B **76**, 045302 (2007).
[3] H. Zhang, C. X. Liu, X. L. Dai, Z. Fang, and S. C. Zhang, Nat. Phys. **5**, 438 (2009).
[4] M. König, S. Wiedmann, C. Brüne, A. Roth, H. Buhmann, L. W. Molenkamp, X.-L. Qi, and S.-C. Zhang, Science **318**, 766 (2007).
[5] D. Hsieh, D. Qian, L. Wray, Y. Xia, Y. S. Hor, R. J. Cava, and M. Z. Hasan, Nature (London) **452**, 970 (2008).
[6] Y. Xia, D. Qian, L. Hsieh, D. Wray, A. Pal, H. Lin, A. Bansil, D. Grauer, Y. S. Hor, R. J. Cava, and M. Z. Hasan, Nat. Phys. **5**, 398 (2009).
[7] A. Altland and M. R. Zirnbauer, Phys. Rev. B **55**, 1142 (1997).
[8] A. Kitaev, *Advances in Theoretical Physics: Landau Memorial Conference*, AIP Conf. Proc. 1134, edited by Lebedev and Mikhail Feigel'man (AIP, Melville, NY, 2009), p. 22.
[9] S. Ryu, A. P. Schnyder, A. Furusaki, and A. W. W. Ludwig, New J. Phys. **12**, 065010 (2010).
[10] M. Dzero, K. Sun, V. Galitski, and P. Coleman, Phys. Rev. Lett. **104**, 106408 (2010).
[11] M. Dzero, K. Sun, P. Coleman, and V. Galitski, Phys. Rev. B **85**, 045130 (2012).
[12] M. Dzero, J. Xia, V. Galitski, and P. Coleman, arXiv:1506.05635.
[13] N. Read and D. M. Newns, J. Phys. C **16**, 3273 (1983).
[14] P. Coleman, Phys. Rev. B **35**, 5072 (1987).
[15] D. M. Newns and N. Read, Adv. Phys. **36**, 799 (1987).
[16] S. Wolgast, C. Kurdak, K. Sun, J. W. Allen, D.-J. Kim, and Z. Fisk, Phys. Rev. B **88**, 180405 (2013).
[17] X. Zhang, N. P. Butch, P. Syers, S. Ziemak, R. L. Greene, and J. Paglione, Phys. Rev. X **3**, 011011 (2013).
[18] N. Xu, P. K. Biswas, J. H. Dil, R. S. Dhaka, G. Landolt, S. Muff, C. E. Matt, X. Shi, N. C. Plumb, M. Radović *et al.*, Nat. Commun. **5**, 4566 (2014).
[19] D. J. Kim, J. Xia, and Z. Fisk, Nat. Mater. **13**, 466 (2014).
[20] V. Alexandrov and P. Coleman, Phys. Rev. B **90**, 115147 (2014).
[21] O. Zachar, S. A. Kivelson, and V. J. Emery, Phys. Rev. Lett. **77**, 1342 (1996).
[22] A. E. Sikkema, I. Affleck, and S. R. White, Phys. Rev. Lett. **79**, 929 (1997).
[23] O. Zachar and A. M. Tsvelik, Phys. Rev. B **64**, 033103 (2001).
[24] H. Tsunetsugu, Y. Hatsugai, K. Ueda, and M. Sigrist, Phys. Rev. B **46**, 3175 (1992).
[25] N. Shibata, T. Nishino, K. Ueda, and C. Ishii, Phys. Rev. B **53**, R8828 (1996).
[26] N. Shibata, A. Tsvelik, and K. Ueda, Phys. Rev. B **56**, 330 (1997).
[27] H. Tsunetsugu, M. Sigrist, and K. Ueda, Rev. Mod. Phys. **69**, 809 (1997).
[28] N. Shibata and K. Ueda, J. Phys.: Condens. Matter **11**, R1 (1999).
[29] O. Zachar, Phys. Rev. B **63**, 205104 (2001).
[30] E. Berg, E. Fradkin, and S. A. Kivelson, Phys. Rev. Lett. **105**, 146403 (2010).
[31] A. Dobry, A. Jaefari, and E. Fradkin, Phys. Rev. B **87**, 245102 (2013).
[32] G. Y. Cho, R. Soto-Garrido, and E. Fradkin, Phys. Rev. Lett. **113**, 256405 (2014).
[33] A. M. Lobos, A. O. Dobry, and V. Galitski, Phys. Rev. X **5**, 021017 (2015).
[34] I. Affleck, T. Kennedy, E. H. Lieb, and H. Tasaki, Phys. Rev. Lett. **59**, 799 (1987).
[35] I. Affleck, T. Kennedy, E. H. Lieb, and H. Tasaki, Commun. Math. Phys. **115**, 477 (1989).
[36] T. Kennedy and H. Tasaki, Phys. Rev. B **45**, 304 (1992).
[37] Z.-C. Gu and X.-G. Wen, Phys. Rev. B **80**, 155131 (2009).
[38] X. Chen, Z.-C. Gu, and X.-G. Wen, Phys. Rev. B **83**, 035107 (2011).
[39] F. Pollmann, E. Berg, A. M. Turner, and M. Oshikawa, Phys. Rev. B **85**, 075125 (2012).
[40] S. R. White, Phys. Rev. Lett. **69**, 2863 (1992).
[41] S. R. White, Phys. Rev. B **48**, 10345 (1993).
[42] A. Luther and I. Peschel, Phys. Rev. B **12**, 3908 (1975).

[43] T. Giamarchi, *Quantum Physics in One Dimension* (Oxford University Press, Oxford, 2004).
[44] S. R. White and D. A. Huse, Phys. Rev. B **48**, 3844 (1993).
[45] D. J. Garcia, K. Hallberg, B. Alascio, and M. Avignon, Phys. Rev. Lett. **93**, 177204 (2004).
[46] M. den Nijs, Phys. Rev. B **46**, 10386 (1992).
[47] G. Wirth, M. Ölschläger, and A. Hemmerich, Nat. Phys. **7**, 147 (2011).
[48] P. Soltan-Panahi, D.-S. Lühmann, J. Struck, P. Windpassinger, and K. Sengstock, Nat. Phys. **8**, 71 (2012).
[49] M. Lewenstein and W. V. Liu, Nat. Phys. **7**, 101 (2011).
[50] X. Li, E. Zhao, and V. Liu, Nat. Commun. **4**, 1523 (2013).
[51] B. Liu, X. Li, R. G. Hulet, and W. V. Liu, arXiv:1505.08164.
[52] H. Chen, X.-J. Liu, and X. C. Xie, arXiv:1509.02893.
[53] U. Schneider, L. Hackermüller, S. Will, T. Best, I. Bloch, T. A. Costi, R. W. Helmes, D. Rasch, and A. Rosch, Science **322**, 1520 (2008).
[54] R. Jördens, N. Strohmaier, K. Günter, H. Moritz, and T. Esslinger, Nature (London) **455**, 204 (2008).
[55] M. Foss-Feig, M. Hermele, and A. M. Rey, Phys. Rev. A **81**, 051603 (2010).
[56] M. Foss-Feig, M. Hermele, V. Gurarie, and A. M. Rey, Phys. Rev. A **82**, 053624 (2010).